



**HAL**  
open science

**Liver mitochondrial coupling efficiency and its  
relationship to adenine nucleotide translocase content:  
A comparative study among crocodiles, birds and  
mammals**

Damien Roussel, Nathan Roussel, Yann Voituron, Benjamin Rey

► **To cite this version:**

Damien Roussel, Nathan Roussel, Yann Voituron, Benjamin Rey. Liver mitochondrial coupling efficiency and its relationship to adenine nucleotide translocase content: A comparative study among crocodiles, birds and mammals. *Mitochondrion*, 2024, 78, 10.1016/j.mito.2024.101909. hal-04648886

**HAL Id: hal-04648886**

**<https://cnrs.hal.science/hal-04648886v1>**

Submitted on 15 Jul 2024

**HAL** is a multi-disciplinary open access archive for the deposit and dissemination of scientific research documents, whether they are published or not. The documents may come from teaching and research institutions in France or abroad, or from public or private research centers.

L'archive ouverte pluridisciplinaire **HAL**, est destinée au dépôt et à la diffusion de documents scientifiques de niveau recherche, publiés ou non, émanant des établissements d'enseignement et de recherche français ou étrangers, des laboratoires publics ou privés.

1 **Liver mitochondrial coupling efficiency and its relationship to adenine nucleotide**  
2 **translocase content: A comparative study among crocodiles, birds and mammals**

3  
4 Damien Roussel<sup>1\*</sup>, Nathan Roussel<sup>2</sup>, Yann Voituron<sup>1</sup>, Benjamin Rey<sup>3</sup>

5  
6 1. Université Claude Bernard Lyon 1, CNRS, ENTPE, UMR 5023 LEHNA, France

7 2. Université Savoie Mont-Blanc, France

8 3. Université Claude Bernard Lyon 1, CNRS, UMR 5558 LBBE, France

9  
10 \*Corresponding authors: LEHNA, UMR 5023 CNRS, Université Claude Bernard Lyon 1,  
11 Bâtiment Charles Darwin C, 69622 Villeurbanne cedex, France.

12 E-mail address: [damien.roussel@univ-lyon1.fr](mailto:damien.roussel@univ-lyon1.fr)

13  
14  
15 **Keywords:** Oxidative phosphorylation, Liver, Adenine nucleotide translocase (ANT), Proton  
16 leak, Archosaurs

## 19 **Summary**

20 The primary objective of this study was to assess whether adenine nucleotide translocase (ANT)  
21 content could be associated with phylogenetic disparities in mitochondrial coupling efficiency,  
22 within liver mitochondria obtained from rats, crocodiles, and ducklings. Our measurements  
23 included mitochondrial membrane conductance, ANT content, and oxidative phosphorylation  
24 fluxes at various steady-state rates. We observed significant variations in ANT content in liver  
25 mitochondria across the three species, and these variations correlated with interspecific  
26 differences in mitochondrial oxidative phosphorylation activity and coupling efficiency. These  
27 findings expand upon previous research by highlighting the pivotal role of ANT in modulating  
28 mitochondrial efficiency on an interspecific scale.

29

## 30 **1. Introduction**

31 Thyroid hormone levels, temperature, and body size represent major determinants of the  
32 mitochondrial oxidative phosphorylation activity and coupling efficiency, deeply ingrained in  
33 phylogenetics. For instance, mitochondria from endothermic vertebrates demonstrate higher  
34 mitochondrial proton conductance compared to ectotherms (Brand et al., 1991; Brookes et al.,  
35 1998; Hulbert et al., 2002; Polymeropoulos et al., 2017). This proton conductance activity,  
36 which does not generate ATP, can lower mitochondrial coupling efficiency, i.e., the ATP/O  
37 ratio, and consequently increase the energy expenditure for mitochondrial ATP synthesis. In  
38 conjunction with greater mitochondrial oxidative and enzyme activities (Bennett, 1972;  
39 Akhmerov, 1986; Paital and Samanta, 2013; Wiens et al., 2017; see however Berner, 1999),  
40 these findings suggest that mitochondria from endotherms convert energy from reduced  
41 coenzymes into ATP at a higher energy cost than ectotherms. However, it was reported that the  
42 contribution of proton leak to the resting metabolic rate of hepatocytes is as high in endotherms  
43 as it is in ectotherms (Brand et al., 1991; Stuart et al., 2001; Hulbert et al., 2002), suggesting

44 similar mitochondrial coupling efficiency, and ultimately, no substantial difference in the cost  
45 of mitochondrial ATP synthesis in cells. Furthermore, the proportion of cellular oxygen  
46 consumption allocated to mitochondrial proton leak (Porter and Brand, 1995; Else et al., 2004a),  
47 as well as the maximal effective coupling efficiency of mitochondria (Boël et al., 2019; Boël et  
48 al., 2023; Barbe et al., 2023), remains similar in birds and mammals regardless of their size,  
49 despite the negative correlation between mitochondrial proton conductance negatively and  
50 body mass in these endothermic species (Porter and Brand, 1993; Brand et al., 2003). All these  
51 data indicate that phylogenetic or allometric differences in the magnitude of mitochondrial  
52 proton conductance may not necessarily lead to alterations in mitochondrial coupling  
53 efficiency, i.e., in the energy cost of ATP production.

54 Mitochondrial coupling efficiency can also be influenced by other characteristics of the  
55 mitochondrial function capable of altering the proton motive force, thus the proton leak activity  
56 across the inner mitochondrial membrane. These characteristics may include, among others,  
57 oxidative capacity (Nogueira et al., 2001; Roussel et al., 2018) or the abundance of  
58 mitochondrial anion carrier proteins such as adenine nucleotide translocase (ANT) (Schönfeld,  
59 1990; Cadenas et al., 2000; Brand et al., 2005; Bertholet et al., 2019). For instance, previous  
60 research has indicated that mitochondrial contents of cytochrome-c oxidase (e.g., cytochrome  
61 a) and ANT contribute to interspecific variations in mitochondrial function (Guderley et al.,  
62 2005; Hulbert et al., 2006). Expanding upon these observations, we examined whether ANT  
63 content could be linked to phylogenetical differences in mitochondrial coupling efficiency, i.e.,  
64 the ATP/O ratio, in liver mitochondria isolated from rats (*Rattus norvegicus*), crocodiles  
65 (*Crocodylus niloticus*), and ducklings (*Cairina moschata*). We assessed the capacity for  
66 succinate oxidation in these mitochondria, measuring their membrane proton conductance and  
67 ANT content. Additionally, we quantified oxygen consumption, ATP synthesis, and the  
68 resulting coupling efficiency (ATP/O ratios) at both maximal and submaximal oxidative

69 phosphorylation rates. Our findings reveal that liver mitochondria from crocodiles display high  
70 coupling efficiency and low inner membrane proton conductance compared to rat mitochondria.  
71 Conversely, rats demonstrate high coupling efficiency and similar inner membrane proton  
72 conductance when compared to duckling mitochondria. These interspecific variations in  
73 mitochondrial coupling efficiency can be attributed to differences in mitochondrial ANT  
74 content.

75

## 76 **2. Materials and methods**

### 77 *2.1. Animals*

78 In the present work, animals of similar body weight were used to limit confounding allometric  
79 effects on liver mitochondrial bioenergetics as described in endotherms and ectotherms (Porter  
80 and Brand, 1993; Brand et al., 2003; Roussel et al., 2015; Boël et al., 2023). Nile crocodiles of  
81 approximately 12-week old (*Crocodylus niloticus*) were captive-bred juveniles kindly donated  
82 by a crocodile farm (Pierrelatte, France). Crocodiles were chosen because their mitochondria  
83 can be assayed at high temperature (Guderley and Seebacher, 2011). They were maintained at  
84 28-30°C for at least 2 weeks prior to the experiments, and were fed on meat. Muscovy ducklings  
85 of ~ 2-week old (*Cairina moschata*) were obtained at the age of 1 day from a commercial  
86 stockbreeder (Ecllosion Grimaud Frères, Roussay, France), maintained at thermoneutrality for  
87 at least 10 days, and fed *ad libitum*. Sprague-Dawley rats (~ 6-week old) were housed in cages  
88 at ~25°C and fed *ad libitum*. All animals had access to water *ad libitum*.

89

### 90 *2.2. Mitochondrial isolation*

91 Liver mitochondria were isolated at 4°C by differential centrifugation as previously described  
92 (Salin et al., 2010; Roussel et al., 2015). We focus our study on liver because that organ  
93 performs identical physiological function and contributes to a significant part of the resting

94 metabolic rate in the three species. In addition, a large amount of mitochondria can be isolated  
95 from this organ, which was necessary to perform the different biochemical protocols described  
96 below. Liver was rapidly dissected, weighed, and homogenized with a Potter-Elvehjem  
97 homogenizer (3 passages) in ice-cold isolation buffer (250 mM sucrose, 1 mM EGTA, 20 mM  
98 Tris-base, and pH 7.3 at 4°C). For crocodile, liver samples from two individuals were pooled  
99 for each mitochondrial preparation. The liver homogenate was centrifuged at 800×g for 10 min.  
100 The supernatant was centrifuged at 1000×g for 10 min, filtered and re-centrifuged at 8,700×g  
101 for 10 min to pellet mitochondria. The mitochondrial pellet was re-suspended in ice-cold  
102 isolation buffer and re-centrifuged twice at 8,700×g for 10 min. The final pellet was re-  
103 suspended in 100 µL isolated buffer and protein content of mitochondrial suspension was  
104 assayed at 540 nm using the biuret method with bovine serum albumin used as standard. Of  
105 note, the mitochondrial preparation from crocodile liver contained a dark pigment which  
106 absorbs at 540 nm. Therefore, for each sample, the absorbance of the same volume of  
107 mitochondria assayed in Biuret solution without copper sulfate (i.e. 0.6% K-Na-tartrate and 3%  
108 NaOH) was used as a blank.

109

### 110 *2.3. Mitochondrial oxidative phosphorylation activity and efficiency*

111 Mitochondrial oxidative phosphorylation efficiency was assessed at 37°C by measuring the  
112 rates of oxygen consumption and ATP synthesis in a respiratory buffer (120 mM KCl, 5 mM  
113 KH<sub>2</sub>PO<sub>4</sub>, 1 mM EGTA, 2 mM MgCl<sub>2</sub>, 0.3 % fatty acid-free bovine serum albumin, 3 mM  
114 HEPES, pH 7.4) supplemented with 1.5 U/ml hexokinase, 20 mM glucose and 5 µM rotenone.  
115 Respiration was initiated by adding succinate (5 mM), then mitochondrial ATP synthesis was  
116 initiated by the addition of 500µM, 100 µM, 25 µM, 10µM or 5 µM ADP. Respiration rates  
117 were measured in a thermostatically regulated glass chamber containing a Clarke-type oxygen  
118 electrode (Rank Brothers Ltd, Cambridge, UK). After recording the phosphorylating respiration

119 rate for at least 2 min, four 300  $\mu$ L samples of mitochondrial suspension were withdrawn from  
120 the suspension every 2 min and were quenched in 200  $\mu$ L perchloric acid solution consisting of  
121 10% HClO<sub>4</sub> and 25 mM EDTA. After centrifugation (15,000 g, 5 min) and neutralization of the  
122 resulting supernatant with a KOH solution (2 M KOH, 0.3 M MOPS), ATP production was  
123 determined from the glucose-6-phosphate content of samples as described previously (Salin et  
124 al., 2010; Roussel et al., 2015). To ensure that mitochondrial rates were specific to  
125 mitochondrial ATP synthase activity, we determined oxygen consumption and ATP synthesis  
126 rates in the presence of oligomycin (2  $\mu$ g/mL). These values were taken into account to calculate  
127 the rate of mitochondrial ATP synthesis. The maximal activity of the electron transport system  
128 was measured as the carbonyl-cyanide *p*-(trifluoromethoxy)phenylhydrazone (FCCP)-induced  
129 maximal respiration rate in mitochondria respiring on succinate (5 mM) in the presence of 5  
130  $\mu$ M rotenone and 2  $\mu$ g/mL oligomycin.

131

#### 132 *2.4. ANT content of mitochondria*

133 The ANT content was determined by titrating the rate of phosphorylating respiration with  
134 increasing concentrations of carboxyatractyloside, an irreversible inhibitor of ANT activity.  
135 Mitochondria (1.35  $\pm$  0.17 mg/mL for crocodile, 0.76  $\pm$  0.11 mg/mL for rat, and 0.50  $\pm$  0.01  
136 mg/mL for ducklings) were incubated in respiratory buffer supplemented with 1.5 U/mL  
137 hexokinase, 20 mM glucose, and energized with 5 mM succinate in the presence of 5  $\mu$ M  
138 rotenone. After 3-5 minutes, 100  $\mu$ M ADP was added to initiate phosphorylating respiration.

139 The mitochondrial content of ANT protein was determined by the amount of  
140 carboxyatractyloside required to completely inhibit the rate of phosphorylating respiration  
141 (Schönfeld, 1990; Roussel et al., 2000).

142

#### 143 *2.5. Mitochondrial membrane potential*

144 Mitochondrial respiration and membrane potential were measured at 37°C in respiratory buffer  
145 supplemented with 5 µM rotenone, 2.5 µg/mL oligomycin, 60 ng/mL nigericin, 2 µM triphenyl-  
146 methyl-phosphonium (TPMP<sup>+</sup>). The TPMP<sup>+</sup> electrode was calibrated by four sequential 0.5 µM  
147 additions of TPMP<sup>+</sup>, then 5 mM succinate was added to start the reaction. The kinetic response  
148 of proton leak to proton-motive force was determined by titration of oxygen consumption with  
149 malonate, up to 10 mM (Salin et al., 2010; Roussel et al., 2018). Membrane potentials were  
150 calculated as previously described by Brand (1995), assuming a TPMP<sup>+</sup>-binding correction of  
151 0.42, 0.54 and 0.66 (µL/mg of protein)<sup>-1</sup> for liver mitochondria of rats, ducklings and crocodiles,  
152 respectively (Brookes et al., 1998; Hulbert et al., 2002; Brand et al., 2003).

153

#### 154 *2.6. Statistical analysis*

155 Data were tested with analysis of variance (ANOVA) for independent values, followed by  
156 protected least significance tests (Staview v4.5 statistical software). The relation between some  
157 of the mitochondrial parameters and the mitochondrial content of ANT was compared using  
158 linear regression. Data are reported as means ± S.E.M. with significance considered at  $p < 0.05$ .

159

### 160 **3. Results and Discussion**

161 Table 1 provides information on the body weight and liver mass of the animals. As  
162 expected (Else and Hulbert, 1985), the liver mass relative to body weight was lower in  
163 crocodiles than in rats or ducklings. Fig. 1A shows that the steady state rates of ADP-induced  
164 phosphorylating oxygen consumption were significantly different between species, being the  
165 lowest in crocodiles and the highest in ducklings. These disparities in the phosphorylating  
166 respiration among species were associated with variations in the maximal respiratory capacity  
167 of mitochondria, as determined by FCCP-induced maximal uncoupled respiration (Fig. 1B).  
168 These findings align with comparative studies that have reported lower mitochondrial activity



169 in ectotherms compared to endotherms (Akhmerov, 1986; Hulbert et al., 2002; Guderley et al.,  
170 2005; Paital and Samanta, 2013; Wiens et al., 2017; see however Berner, 1999). Thyroid  
171 hormone level and membrane lipid composition are among mechanisms well known to cause  
172 variation in metabolic rate and mitochondrial activity (Brookes et al., 1998; Nogueira et al.,  
173 2002; Brand et al., 2003). Hence, a lower level of thyroid hormones and/or a lower proportion  
174 of docosahexanoic acid (C22:6n-3) within membrane are mechanisms able to cause lower  
175 mitochondrial activity in crocodiles compared to endotherms. Interestingly, these mechanisms  
176 are, more generally, involved in the evolution of endothermy (Else et al., 2004b; Little and  
177 Seebacher, 2014).

178 Fig. 2A reports the linear relationship between the rates of ATP synthesis and oxygen  
179 consumption in liver mitochondria from crocodiles, rats, and ducklings. The maximal rates of  
180 ATP synthesis and the corresponding oxygen consumption (i.e., the highest points on the right  
181 side of the linear relationships in Fig. 2A) were lowest in crocodiles and highest in ducklings,  
182 with the order being crocodile < rat < duckling. Crocodile mitochondria exhibited  
183 approximately 2.5 and 3.5 times lower rates of ATP synthesis and oxygen consumption,  
184 respectively, compared to rat and duckling mitochondria. The slopes of the linear relationships  
185 did not show significant differences between species ( $P/O_{\text{crocodile}} = 1.54 \pm 0.12$ ;  $P/O_{\text{rat}} = 1.34 \pm$   
186  $0.06$ ;  $P/O_{\text{duckling}} = 1.36 \pm 0.04$ ;  $p=0.18$ ), indicating that these relationships were parallel.  
187 However, the rates of non-phosphorylating respiration (the points where the curves intersect the  
188  $x$ -axis) significantly varies among the three species (crocodile < rat < duckling; see Table 1 and  
189 Fig. 2A). Consequently, the linear curves for crocodile mitochondria and duckling  
190 mitochondria were notably shifted to the left and right, respectively, compared to the curve for  
191 rat mitochondria (Fig. 2A). This suggests that at any given steady-state rate of ATP production,  
192 crocodile liver mitochondria consumed less oxygen, whereas duckling mitochondria required  
193 more oxygen than rat mitochondria. This difference is better illustrated in Fig. 1B, which shows

194 that for any given rate of oxygen uptake, the ATP/O of liver mitochondria was higher in  
195 crocodiles and lower in ducklings compared to rats. Overall, crocodile liver mitochondria  
196 exhibited greater efficiency, whereas duckling mitochondria displayed lower efficiency than rat  
197 mitochondria (Fig. 2). In the present work, we used juveniles that were of the same body mass  
198 but not of the same age due to growth rate differences between species. In juvenile brown trout,  
199 it has been shown that individuals with a higher growth performance also exhibited a higher  
200 coupling efficiency in their liver mitochondria (Salin et al., 2019). In common frog, an  
201 intraspecies comparison of populations having large differences in body mass at the same age  
202 found that frogs with high growth rates and large body sizes exhibited higher mitochondrial  
203 coupling efficiency compared to the smaller frogs (Salin et al., 2012). In contrast, differences  
204 in growth performance in broilers were not associated with mitochondrial efficiency variations  
205 in skeletal muscle and liver (Bottje et al., 2002). In rat, values of thermodynamic efficiency of  
206 liver mitochondrial oxidative phosphorylation did not seem to vary in 40- to 180-day-old rats  
207 (Lionetti et al., 2004; Iossa et al., 1998). In endotherms. Altogether these studies suggest that  
208 in the present study, the difference in stage of development between juveniles would not fully  
209 explain differences in mitochondrial coupling efficiency between the three species.

210 As shown in Fig. 2B, the effective ATP/O ratio displays a non-linear relationship with  
211 mitochondrial oxidative activity. It increases sharply as the phosphorylation rate rises before  
212 leveling off and reaching a maximum. This non-linear relationship results from the fact that  
213 proton leak pathways and ATP synthesis compete for the same driving force, known as the  
214 proton motive force (Brand, 2005). Consequently, during the dynamic transition from the basal  
215 non-phosphorylating state to the maximal phosphorylating state (Fig. 2), proton leak  
216 significantly decreases as oxidative phosphorylation increases, leading to better mitochondrial  
217 efficiency (ATP/O ratio). Therefore, there is no fixed value for the ATP/O ratio that can  
218 describe effective coupling efficiency, as it closely depends on the degree of oxidative

219 phosphorylation activity. Nonetheless, this non-linear mitochondrial property can be quantified  
220 by fitting the relationships between ATP/O ratios and the rates of oxygen consumption with a  
221 mono-exponential function  $[ATP/O = ATP/O_{max} \times (1 - e^{-mtEC \times (J_O - J_{O_{basal}})})]$ ; Mogensen and Sahlin,  
222 2005], where  $J_O$  represents the phosphorylating oxygen consumption rate,  $J_{O_{basal}}$  is the non-  
223 phosphorylating oxygen consumption rate (the intersection point with the  $x$ -axis), and “mtEC”  
224 is the gradient of the non-linear curve. This factor has been termed the mitochondrial efficiency  
225 channeling (mtEC) factor because it describes how rapidly mitochondrial coupling efficiency  
226 reaches its maximum. The mtEC factor value can then be used as a single mitochondrial  
227 parameter to describe the overall variation in effective coupling efficiency with changes in  
228 mitochondrial activity or power (Boël et al., 2019). In the present study, mtEC was highest in  
229 crocodiles and lowest in ducklings (Fig. 2B inset). These results show that the increase in  
230 effective ATP/O ratios was steeper, indicating better coupling in crocodiles than in ducklings,  
231 with rat mitochondria falling in between.

232 Differences in mitochondrial proton conductance may contribute to variations in  
233 mitochondrial coupling efficiency (Beavis and Lehninger, 1986; Brand et al., 1991; Nogueira  
234 et al., 2002). This is supported by the fact that the shifts in the relationships depicted in Fig. 2  
235 seem to be driven by differences in the rates of non-phosphorylating respiration, a respiratory  
236 state characterized by the absence of ATP synthesis, a high proton motive force, and maximal  
237 proton leakage (Brand and Nicholls, 2011). In the present study, the inner membrane proton  
238 conductance of liver mitochondria was higher in rats than in crocodiles (Fig. 1S.A), but there  
239 was no significant difference between rats and ducklings (Fig. 1S.B). At comparable potential  
240 values, the permeability of the inner membrane to protons was approximately three times  
241 greater in rats than in crocodiles. These results align with previous studies that have shown that  
242 mitochondria from small reptile species (< 2-3 kg) exhibit lower proton conductance than  
243 mitochondria from mammals of similar body weight (Brand et al., 1991; Brookes et al., 1998).

244 It is worth noting that these differences between reptiles and mammals are less pronounced  
245 when comparing larger species (Hulbert et al., 2002; Polymeropoulos et al., 2017). Further  
246 insight, the higher proton conductance in rat mitochondria was associated with a lower value  
247 of effective ATP/O ratio at maximal phosphorylating activities (the highest points to the right  
248 of the non-linear curve in Fig. 2B) than in crocodile mitochondria ( $ATP/O_{Rat} = 1.14 \pm 0.05$   
249 versus  $ATP/O_{Crocodile} = 1.26 \pm 0.11$ ). Although the difference did not reach significance, this  
250 result aligns with previous studies showing that agents that increase mitochondrial proton  
251 conductance, such as thyroid hormones or mitochondrial uncouplers, also decrease the effective  
252 coupling efficiency at maximal phosphorylating activity (Beavis and Lehninger, 1986;  
253 Nogueira et al., 2001; Nogueira et al., 2002). Taken together, these observations suggest that  
254 differences in membrane conductance to protons may partly explain the differences in  
255 mitochondrial efficiency between crocodiles and rats. In contrast to ectothermic species,  
256 mitochondrial proton conductance is less distinct between bird and mammal species (Brookes  
257 et al., 1998; Brown et al., 2009; Polypopoulos et al., 2017). In the present study, the  
258 mitochondrial inner membrane proton conductance was not different between rats and  
259 ducklings (Fig. 1S.B). This result implies that difference in coupling efficiency between rats  
260 and ducklings was mainly linked to a difference in the mitochondrial oxidative capacity. This  
261 hypothesis is largely supported by previous studies showing that mitochondria with a lower  
262 oxidative phosphorylation capacity often exhibit a higher coupling efficiency, such as in the  
263 presence of low dose of cyanide or nitric oxide or following caloric restriction (Zangarelli et  
264 al., 2006; Clerc et al., 2007; Roussel et al., 2018).

265 The mitochondrial coupling efficiency (ATP/O ratio) is not only negatively controlled  
266 by proton leak, but also by its sensitivity to changes in phosphorylation reactions, which exert  
267 roughly equal positive control. These reactions encompass several steps, including those  
268 involving the ATP synthase, the phosphate carrier, and the ANT (Brand et al., 1993; Roussel et

269 al., 2004). ANT is a major transport protein located in the inner mitochondrial membrane,  
270 supplying the cell with ATP during periods of high energy demand. Previous research has  
271 reported a correlation between ANT content correlates and interspecific variations in  
272 mitochondrial oxidative capacity in muscle mitochondria (Guderley et al., 2005). In the present  
273 study, the ANT content in liver mitochondria differed significantly among the three species,  
274 with the lowest content observed in crocodiles and the highest in ducklings (crocodile < rat <  
275 duckling; see Fig. 3).

276 While ANT's primary role is to export ATP from the mitochondrial matrix to the cytosol  
277 while importing cytosolic ADP when cellular energy needs are high, it can also catalyze proton  
278 leakage in the resting state when cellular energy needs are low (Bertholet et al., 2019). In  
279 addition, ANT can also facilitate fatty acid- or AMP-induced uncoupling in resting  
280 mitochondria (Schönfeld, 1990; Roussel et al., 2000; Cadenas et al., 2000; [Bottje et al., 2009](#);  
281 [Guderley and Seebacher, 2011](#)). It has also been reported that ANT may contribute from half  
282 to two-thirds of the basal proton conductance in resting mitochondria (Brand et al., 2005). In  
283 the present study, the basal non-phosphorylating state of respiration, measured in the presence  
284 of oligomycin, was sensitive to CAT addition (Table 1). Based on these data, we can estimate  
285 that ANT may contribute to more than half of the basal non-phosphorylating respiration rate in  
286 rats, which was significantly higher than the values calculated in crocodiles and ducklings  
287 (Table 1). The basal non-phosphorylating respiration serve as a measure of the maximal proton  
288 leakage across the inner mitochondrial membrane. Hence, these data suggest that differences in  
289 mitochondrial ANT content may drive part of the differences in coupling efficiency between  
290 species. This hypothesis is reinforced by the fact that, when mitochondrial fluxes (ATP  
291 synthesis and corresponding oxygen uptake) are normalized by mitochondrial ANT content,  
292 the relationships between the rates of ATP synthesis and oxygen consumption from crocodiles,  
293 rats and ducklings overlap (Fig. 4). [It must be kept in mind that the present results are based on](#)

294 succinate oxidation. Previous studies have shown that ANT is a major controlling step of the  
295 oxygen-consumption flux in rat liver mitochondria respiring on succinate (Groen et al., 1982;  
296 Kunz et al., 1988; Rossignol et al., 2000). In contrast, it appears that ANT becomes a minor  
297 controlling step of the phosphorylating respiration in mitochondria respiring on  
298 pyruvate/malate (Rossignol et al., 2000). Whether differences in mitochondrial ANT contents  
299 between species would have mediated differences in coupling efficiency of mitochondria  
300 respiring on NADH-linked substrates remain an open question that deserves further  
301 experimental testing.

302 In conclusion, these results offer a comprehensive insight into the variations in oxidative  
303 phosphorylation activity, membrane proton conductance, and coupling efficiency among the  
304 major taxonomic groups. They also expand upon previous research by highlighting the  
305 significant role of ANT in regulating mitochondrial efficiency across different. ~~The question of~~  
306 ~~the evolutionary pressures influencing ANT and the precise mechanisms through which it~~  
307 ~~influences differences in mitochondrial energetics among major taxonomic groups remains~~  
308 ~~unanswered but presents an intriguing avenue for further exploration in this field.~~

309

310

311

312

313

314 **References**

- 315 [1] Akhmerov, R.N. 1986. Qualitative difference in mitochondria of endothermic and  
316 ectothermic animals. *FEBS Lett.* 198, 251-255.
- 317 [2] Barbe, J., Watson, J., Roussel, D., Voituron, Y. 2023. The allometry of mitochondrial  
318 efficiency is tissue-dependent: a comparison between skeletal and cardiac muscles of  
319 birds. *J. Exp. Biol.* 226, jeb246299.
- 320 [3] Beavis, A.D., Lehninger, A.L. 1986. The upper and lower limits of the mechanistic  
321 stoichiometry of mitochondrial oxidative phosphorylation. *Eur. J. Biochem.* 158, 315-  
322 322.
- 323 [4] Bennett, A.F. 1972. A comparison of activities of metabolic enzymes in lizards and rats.  
324 *Comp. Biochem. Physiol.* 42B, 637-647.
- 325 [5] Berner, N.J. 1999. Oxygen consumption by mitochondria from an endotherm and an  
326 ectotherm. *Comp. Biochem. Physiol.* 124B, 25-31.
- 327 [6] Bertholet, A.M., Chouchani, E.T., Kazak, L., Angelin, A., Fedorenko, A., Long, J.Z.,  
328 Vidoni, S., Garrity, R., Cho, J., Terada, N., Wallace, D.C., Spiegelman, B.M., Kirichok,  
329 Y. 2019. H<sup>+</sup> transport is an integral function of the mitochondrial ADP/ATP carrier.  
330 *Nature* 571, 515-520.
- 331 [7] Boël, M., Romestaing, C., Voituron, Y., Roussel, D. 2019. Allometry of mitochondrial  
332 efficiency is set by metabolic intensity. *Proc. R. Soc. B* 286, 20191693.
- 333 [8] Boël, M., Voituron, Y., Roussel, D. 2023. Body mass dependence of oxidative  
334 phosphorylation efficiency in liver mitochondria from mammals. *Comp. Biochem.*  
335 *Physiol.* 284A, 111490.
- 336 [9] Bottje, W., Tang, Z.X., Iqbal, M., Cawthon, D., Okimoto, R., Wing, T., Cooper, M.  
337 2002. Association of mitochondrial function with feed efficiency within single genetic  
338 line of male Broilers. *Poultry Sci.* 81, 546-555.

- 339 [10] Bottje, W., Brand, M.D., Ojano-Dirain, C., Lassiter, K., Toyomizu, M., Wing, T. 2009.  
340 Mitochondrial proton leak kinetics and relationship with feed efficiency within a single  
341 genetic line of male broilers. *Poultry Sci.* 88, 1683-1693.
- 342 [11] Brand, M.D. 1995. Measurement of mitochondrial protonmotive force. In  
343 *Bioenergetics. A practical approach* (Brown, G.C. and Cooper, C.E., eds.), pp. 39-62,  
344 IRL Press, Oxford.
- 345 [12] Brand, M.D. 2005. The efficiency and plasticity of mitochondrial energy transduction.  
346 *Biochem. Soc. Trans.* 33, 897-904.
- 347 [13] Brand, M.D., Couture, P., Else, P.L., Withers, K.W., Hulbert, A.J. 1991. Proton  
348 permeability of the inner membrane of liver mitochondria is greater in a mammal than  
349 in a reptile. *Biochem. J.* 275, 81-86.
- 350 [14] Brand, M.D., Harper, M.E., Taylor, H.C. 1993. Control of the effective P/O ratio of  
351 oxidative phosphorylation in liver mitochondria and hepatocytes. *Biochem. J.* 291, 739-  
352 748.
- 353 [15] Brand, M.D., Turner, N., Ocloo, A, Else, P.L., Hulbert, A.J. 2003. Proton conductance  
354 and fatty acyl composition of liver mitochondria correlates with body mass in birds.  
355 *Biochem. J.* 376, 741-748.
- 356 [16] Brand, M.D., Nicholls, D.G. 2011. Assessing mitochondrial dysfunction in cells.  
357 *Biochem. J.* 435, 297-312.
- 358 [17] Brand, M.D., Pakay, J.L., Ocloo, A., Kokoszka, J., Wallace, D.C., Brookes, P.S.,  
359 Cornwall, E.J. 2005. The basal proton conductance of mitochondria depends on adenine  
360 nucleotide translocase content. *Biochem. J.* 392, 353-362.
- 361 [18] Brookes, P.S., Buckingham, J.A., Tenreiro, A.M., Hulbert, A.J., Brand, M.D. 1998. The  
362 proton permeability of the inner membrane of liver mitochondria from ectothermic and



363 endothermic vertebrates and from obese rats: correlation with standard metabolic rate  
364 and phospholipid fatty acid composition. *Comp. Biochem. Physiol.* 119B, 325-334.

365 [19] Brown, J.C.L., McClelland, G.B., Faure, P.A., Klaiman, J.M., Staples, J.F. 2009.  
366 Examining the mechanisms responsible for lower ROS release rates in liver  
367 mitochondria from long-lived house sparrow (*Passer domesticus*) and big brown bat  
368 (*Eptesicus fuscus*) compared to the short-lived mouse (*Mus musculus*). *Mech. Ageing*  
369 *Dev.* 130, 467-476.

370 [20] Cadenas, S., Buckingham, J.A., St-Pierre, J., Dickinson, K., Jones, R.B., Brand, M.D.  
371 2000. AMP decreases the efficiency of skeletal muscle mitochondria. *Biochem. J.* 351,  
372 307-311.

373 [21] Clerc, P., Rigoulet, M., Leverve, X., Fontaine, E. 2007. Nitric oxide increases oxidative  
374 phosphorylation efficiency. *J. Bioenerg. Biomembr.* 39, 158-166.

375 [22] Else, P.L., Hulbert, A.J. 1985. An allometric comparison of the mitochondria of  
376 mammalian and reptilian tissues: The implications for the evolution of endothermy. *J.*  
377 *Comp. Physiol. B* 156, 3-11.

378 [23] Else, P.L., Brand, M.D., Turner, N., Hulbert, A.J. 2004a. Respiration rate of hepatocytes  
379 varies with body mass in birds. *J. Exp. Biol.* 207, 2305-2311.

380 [24] Else, P.L., Turner, N., Hulbert, A.J. 2004b. The evolution of endothermy: role for  
381 membranes and molecular activity. *Physiol. Biochem. Zool.* 77, 950-958.

382 [25] Groen, A.K., Wanders, R.J.A., Westerhoff, H.V., van der Meer, R., Tager, J.M. 1982.  
383 Quantification of the contribution of various steps to the control of mitochondrial  
384 respiration. *J. Biol. Chem.* 257, 2754-2757.

385 [26] Guderley, H., Turner, N., Else, P.L., Hulbert, A.J. 2005. Why are some mitochondria  
386 more powerful than others: insights from comparisons of muscle mitochondria from  
387 three terrestrial vertebrates. *Comp. Biochem. Physiol.* 142B, 172-180.

- 388 [27] Guderley, H., Seebacher, F. 2011. Thermal acclimation, mitochondrial capacities and  
389 organ metabolic profiles in a reptiles (*Alligator mississippiensis*). *J. Comp. Physiol. B*  
390 181, 53-64.
- 391 [28] Hulbert, A.J., Else, P.L., Manolis, S.C., Brand, M.D. 2002. Proton leak in hepatocytes  
392 and liver mitochondria from archosaurs (crocodiles) and allometric relationships from  
393 ectotherms. *J. Comp. Physiol. B* 172, 387-397.
- 394 [29] Hulbert, A.J., Turner, N., Hinde, J., Else, P., Guderley, H. 2006. How might you  
395 compare mitochondria from different tissues and different species? *J. Comp. Physiol. B*  
396 176, 93-105.
- 397 [30] Iossa, S., Lionetti, L., Mollica, M.P., Barletta, A., Liverini, G. 1998. *Cell Biochem.*  
398 *Funct.* 16, 161-168.
- 399 [31] Kunz, W., Gellerich, F.N., Schild, L., Schönfeld, P. 1988. Kinetic limitations in the  
400 overall reaction of mitochondrial oxidative phosphorylation accounting for flux-  
401 dependent changes in the apparent  $\Delta G^{\text{ex}}_{\text{P}}/\Delta\mu\text{H}^+$  ratio. *FEBS Lett.* 233, 17-21.
- 402 [32] Little, A.G., Seebacher, F. 2014. The evolution of endothermy is explained by thyroid  
403 hormone-mediated responses to cold in early vertebrates. *J. Exp. Biol.* 217, 1642-1648.
- 404 [33] Lionetti, L., Crescenzo, R., Mollica, M.P., Tasso, R., Barletta, A., Liverini, G., Iossa, S.  
405 2004. Modulation of hepatic mitochondrial energy efficiency with age. *Cell. Mol. Life*  
406 *Sci.* 61, 1366-1371.
- 407 [34] Mogensen, M., Sahlin, K. 2005. Mitochondrial efficiency in rat skeletal muscle:  
408 influence of respiration rate, substrate and muscle type. *Acta Physiol. Scand.* 185, 229-  
409 236.
- 410 [35] Nogueira, V., Rigoulet, M., Piquet, MA., Devin, A., Fontaine, E., Leverve, X.M. 2001.  
411 Mitochondrial respiratory chain adjustment to cellular energy demand. *J. Biol. Chem.*  
412 276, 46104-46110.

- 413 [36] Nogueira, V., Walter, L., Avéret, N., Fontaine, E., Rigoulet, M., Leverve, X.M. 2002.  
414 Thyroid status is a key regulator of both flux and efficiency of oxidative  
415 phosphorylation in rat hepatocytes. *J. Bioenerg. Biomembr.* 34, 55-66.
- 416 [37] Paital, B., Samanta, L. 2013. A comparative study of hepatic mitochondrial oxygen  
417 consumption in four vertebrates by using clark-type electrode. *Acta Biol. Hung.* 64,  
418 152-160.
- 419 [38] Polymeropoulos, E.T., Oelkrug, R., White, C.R., Jastroch, M. 2017. Phylogenetic  
420 analysis of the allometry of metabolic rate and mitochondrial basal proton leak. *J.*  
421 *Therm. Biol.* 68, 83-88.
- 422 [39] Porter, R.K., Brand, M.D. 1993. Body mass dependence of H<sup>+</sup> leak in mitochondria and  
423 its relevance to metabolic rate. *Nature* 362, 628-630.
- 424 [40] Porter, R.K., Brand, M.D. 1995. Causes of differences in respiration rate of hepatocytes  
425 from mammals of different body mass. *Am. J. Physiol.* 269, R1213-R1224.
- 426 [41] Rossignol, R., Letellier, T., Malgat, M., Rocher, C., Mazat, J.P. 2000. Tissue variation  
427 in the control of oxidative phosphorylation: implication for mitochondrial diseases.  
428 *Biochem. J.* 347, 45-53.
- 429 [42] Roussel, D., Chainier, F., Rouanet, J.L., Barré, H. 2000. Increase in the adenine  
430 nucleotide translocase content of duckling subsarcolemmal mitochondria during cold  
431 acclimation. *FEBS Lett.* 477, 141-144.
- 432 [43] Roussel, D., Dumas, J.F., Simard, G., Malthièry, Y., Ritz, P. 2004. Kinetics and control  
433 of oxidative phosphorylation in rat liver mitochondria after dexamethasone treatment.  
434 *Biochem. J.* 382, 491-499.
- 435 [44] Roussel, D., Salin, K., Dumet, A., Romestaing, C., Rey, B., Voituron, Y. 2015.  
436 Oxidative phosphorylation efficiency, proton conductance and reactive oxygen species

- 437 production of liver mitochondria correlates with body mass in frogs. *J. Exp. Biol.* 218,  
438 3222-3228.
- 439 [45] Roussel, D., Boël, M., Romestaing, C. 2018. Fasting enhances mitochondrial efficiency  
440 in duckling skeletal muscle by acting on the substrate oxidation system. *J. Exp. Biol.*  
441 221, jeb172213.
- 442 [46] Salin, K., Teulier, L., Rey, B, Rouanet, J.L., Voituron, Y., Duchamp, C., Roussel, D.  
443 2010. Tissue variation of mitochondrial oxidative phosphorylation efficiency in cold-  
444 acclimated ducklings. *Acta. Biochim. Pol.* 57, 409-412.
- 445 [47] Salin, K., Roussel, D., Rey, B., Voituron, Y. 2012. David and Goliath: a mitochondrial  
446 coupling problem? *J. Exp. Zool.* 317, 283-293.
- 447 [48] Salin, K., Villasevil, E.M., Anderson, G.J., Lamarre, S.G., Melanson, C.A., McCarthy,  
448 I., Selman, C., Metcalfe, N.B. 2019. Differences in mitochondrial efficiency explain  
449 individual variation in growth performance. *Proc. R. Soc. B* 2586, 20191466.
- 450 [49] Schönfeld, P. 1990. Does the function of adenine nucleotide translocase in fatty acid  
451 uncoupling depend on the type of mitochondria? *FEBS Lett.* 264, 246-248.
- 452 [50] Stuart, J.A., Cadenas, S., Jekabsons, M.B., Roussel, D., Brand, M.D. 2001.  
453 Mitochondrial proton leak and the uncoupling protein 1 homologues. *Biochim. Biophys.*  
454 *Acta* 1504, 144-158.
- 455 [51] Wiens, L., Banh, S., Sotiri, E., Jastroch, M., Block, B.A., Brand, M.D., Treberg, J.R.  
456 2017. Comparison of mitochondrial reactive oxygen species production of ectothermic  
457 and endothermic fish muscle. *Font. Physiol.* 8, e704.
- 458 [52] Zangarelli, A., Chanseaume, E., Morio, B., Brugère, C., Mosoni, L., Rousset, P.,  
459 Giraudet, C., Patrac, V., Gachon, P., Boirie, Y., Walrand, S. 2006. Synergistic effects  
460 of caloric restriction with maintained protein intake on skeletal muscle performance in  
461 21-month-old rats: a mitochondria-mediated pathway. *FASEB J.* 20, 2439-2450.



463 **Figure Legends**

464 **Figure 1:** Mitochondrial oxidative capacity of liver mitochondria. (A) The rate of oxygen  
465 consumption as a function of ADP concentration from crocodiles (grey diamonds), rats (white  
466 circles), and ducklings (black triangles). (B) Maximal respiratory capacity measured in the  
467 presence of FCCP from crocodiles (grey bar), rats (white bar), and ducklings (black bar). Values  
468 represent means  $\pm$  s.e.m. from (n) independent mitochondrial preparations; (n) is provided  
469 alongside the species name. Overall kinetics (A) or bars (B) with different superscript letters  
470 are significantly different at  $P<0.05$ .

471

472 **Figure 2:** Mitochondrial oxidative phosphorylation activity (A) and efficiency (B) in liver  
473 mitochondria from crocodiles (grey diamonds), rats (white circles), and ducklings (black  
474 triangles). Inset of Panel B: Mitochondrial efficiency channel factor (mtEC; details in text).  
475 Values represent means  $\pm$  s.e.m. from (n) independent mitochondrial preparations; (n) is  
476 provided alongside the species name. Data with different superscript letters are significantly  
477 different at  $P<0.05$ ; In panels A, lower case and upper case letters compare rates of oxygen  
478 consumption and ATP synthesis, respectively. † $P<0.05$ , indicates significant overall  
479 differences in kinetics (see text for details).

480

481 **Figure 3:** ANT content in liver mitochondria from crocodiles (grey diamonds), rats (white  
482 circles), and ducklings (black triangles). (A) Phosphorylating respiration was titrated by  
483 successive additions of carboxyatractyloside (CAT) until maximal inhibition of mitochondrial  
484 respiration was achieved. ANT content was determined by the amount of CAT required for  
485 complete inhibition of phosphorylating respiration. (B) ANT contents measured through CAT  
486 titration. Data with different superscript letters are significantly different at  $P<0.05$ . Values

487 represent means  $\pm$  s.e.m. from (n) independent mitochondrial preparations; (n) is indicated  
488 alongside the species name.

489

490 **Figure 4:** Mitochondrial oxidative phosphorylation efficiency in liver mitochondria from  
491 crocodiles (grey diamonds), rats (white circles), and ducklings (black triangles). The rates of  
492 ATP synthesis and oxygen consumption from Fig. 1A were normalized by the corresponding  
493 ANT contents of mitochondria from Fig. 2B. Values represent means  $\pm$  s.e.m. from (n)  
494 independent mitochondrial preparations; (n) is indicated alongside the species name. \* and †  
495 indicate that the maximal rates of ATP synthesis and oxygen consumption in rats were  
496 significantly different from crocodiles and ducklings ( $P < 0.05$ ).

497

498 **Supplemental Figure 1:** Basal proton conductance of liver mitochondria from crocodiles (grey  
499 diamonds), rats (white circles), and ducklings (black triangles). Proton conductance was  
500 assessed in medium containing rotenone, succinate, oligomycin and nigericin, and membrane  
501 potential and respiration rate were titrated with malonate as described in the “Materials and  
502 Methods” section. Proton leakage rate was calculated from respiration rate by assuming a  $H^+/O$   
503 ratio of 6 for succinate oxidation. Values represent means  $\pm$  s.e.m. from (n) independent  
504 mitochondrial preparations; (n) is given alongside the species name.

505

506 Table 1: Body weight, liver mass and properties of liver mitochondria

	Crocodile (5)	Rat (6)	Duckling (6)
Body weight (g)	143 ± 13 <sup>a</sup>	194 ± 9 <sup>b</sup>	189 ± 14 <sup>b</sup>
Liver (g)	2.9 ± 0.3 <sup>a</sup>	7.4 ± 0.7 <sup>b</sup>	8.5 ± 0.9 <sup>b</sup>
Liver (g/100 BW)	2.0 ± 0.1 <sup>a</sup>	3.8 ± 0.3 <sup>b</sup>	4.6 ± 0.4 <sup>b</sup>
Mitochondrial oxygen consumption (nmol O/min.mg protein)			
Non-phosphorylating rate	10.6 ± 2.3 <sup>a</sup>	19.8 ± 2.7 <sup>b</sup>	30.1 ± 3.6 <sup>c</sup>
CAT-insensitive non-phosphorylating rate <sup>1</sup>	7.5 ± 1.6 <sup>a</sup>	7.9 ± 1.7 <sup>a</sup>	22.3 ± 2.4 <sup>b</sup>
CAT-sensitive respiration (% of non-phosphorylating state) <sup>1</sup>	15 ± 3 <sup>a</sup>	54 ± 7 <sup>b</sup>	21 ± 5 <sup>a</sup>

507 Values are means ± s.em. from (n) independent mitochondrial preparations; (n) is provided alongside the species name. Data with different  
 508 superscript letters are significantly different at P<0.05.

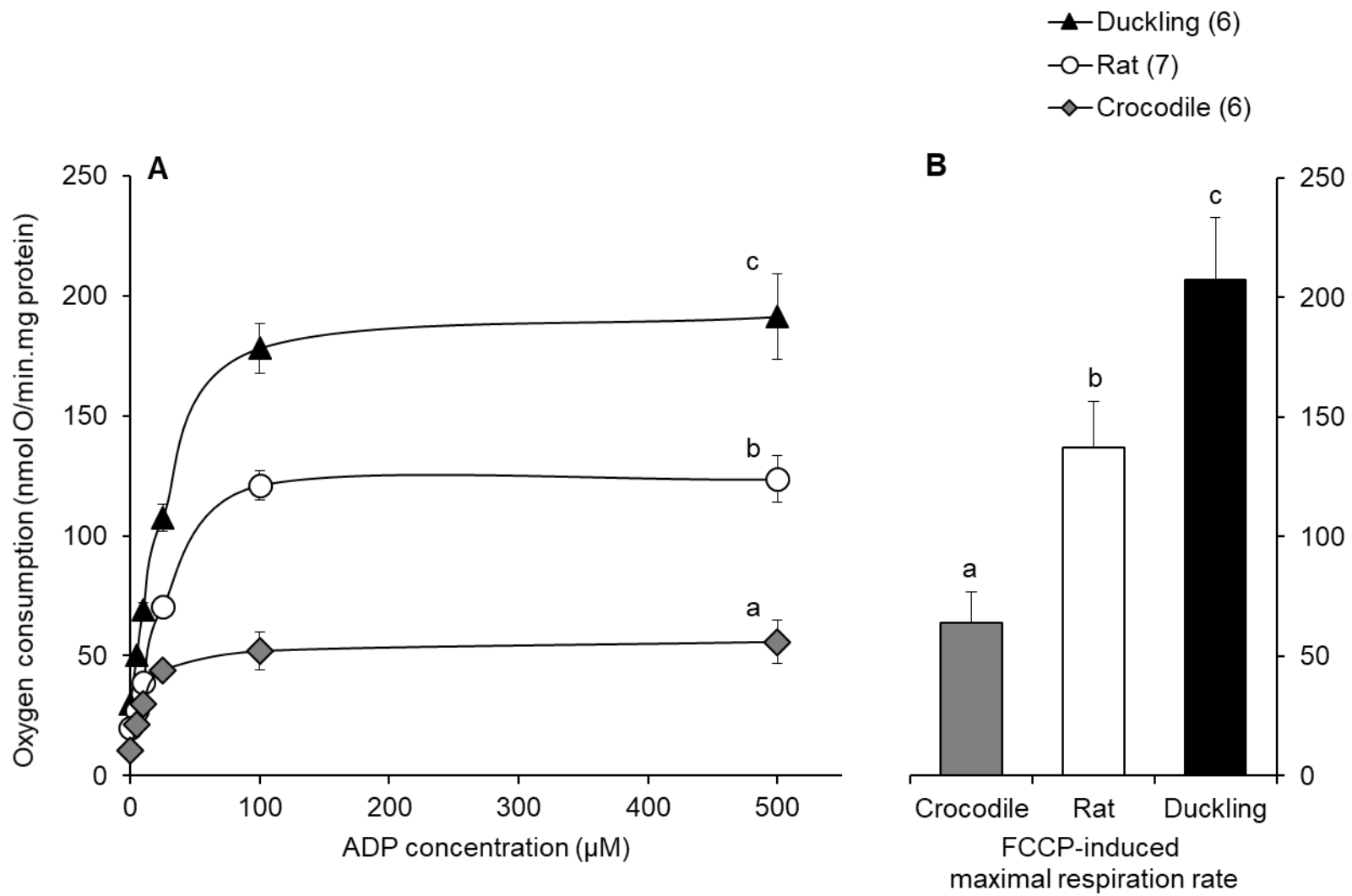
509

510



511  
512

Figure 1



513

Figure 2

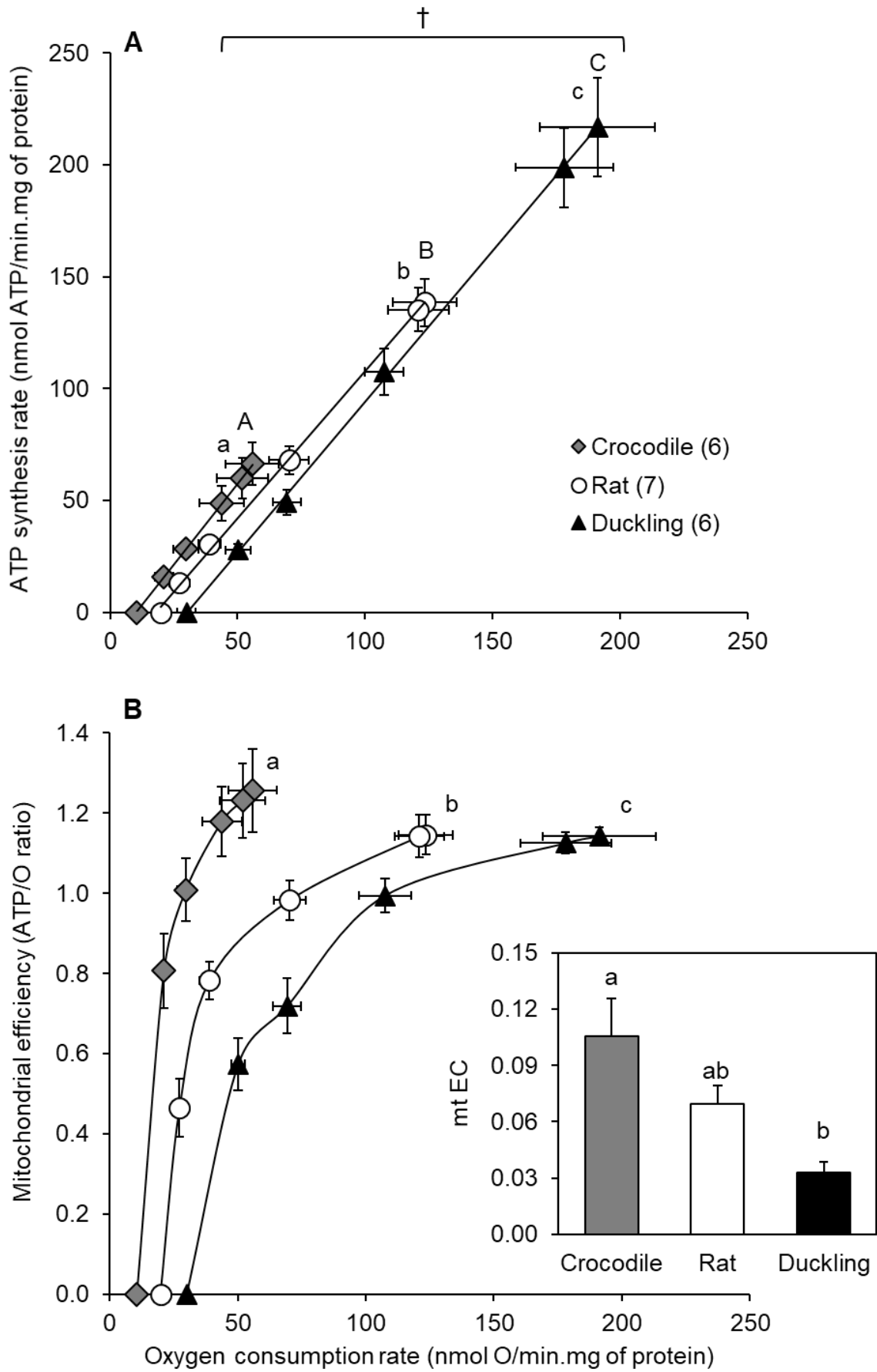


Figure 3

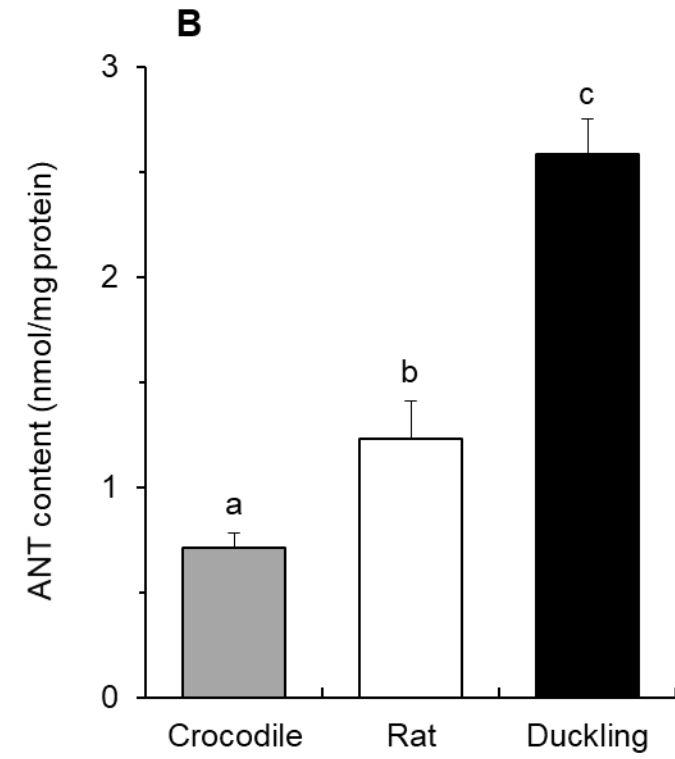
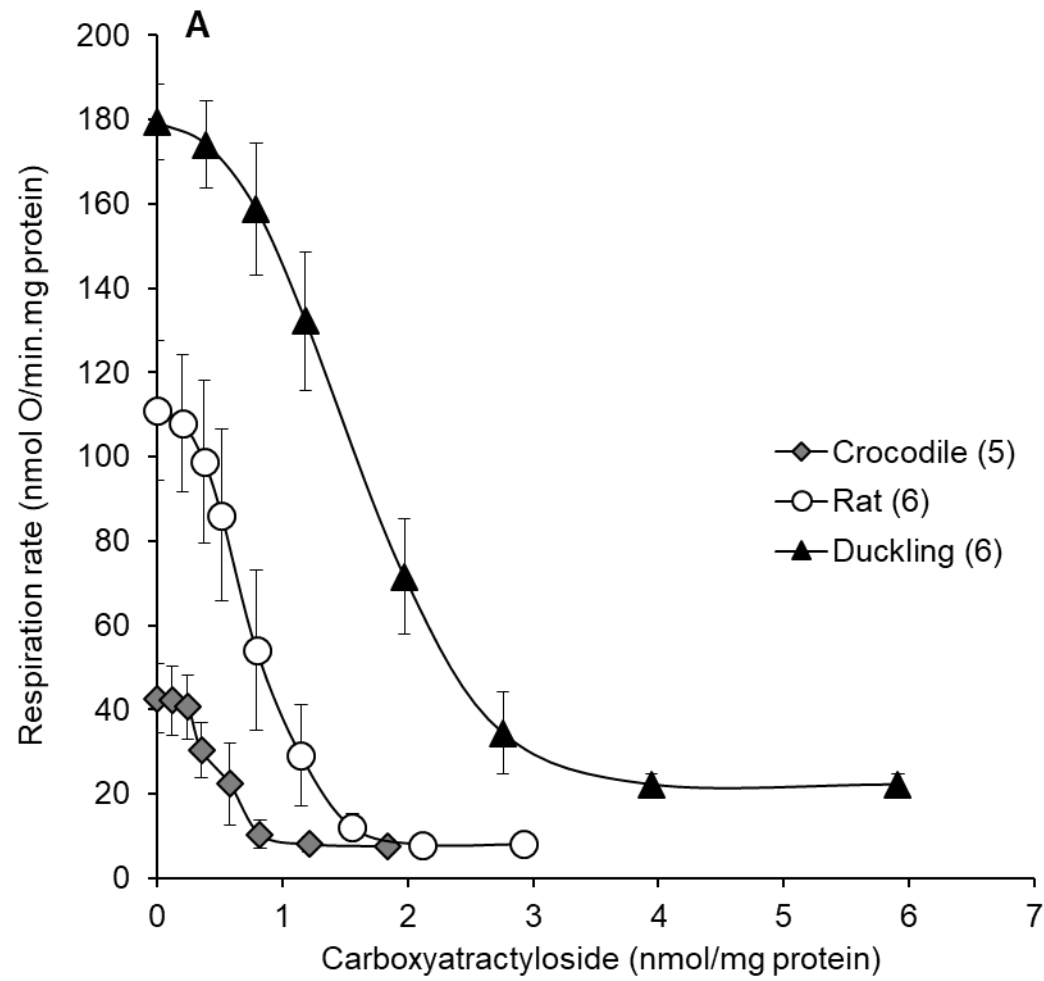
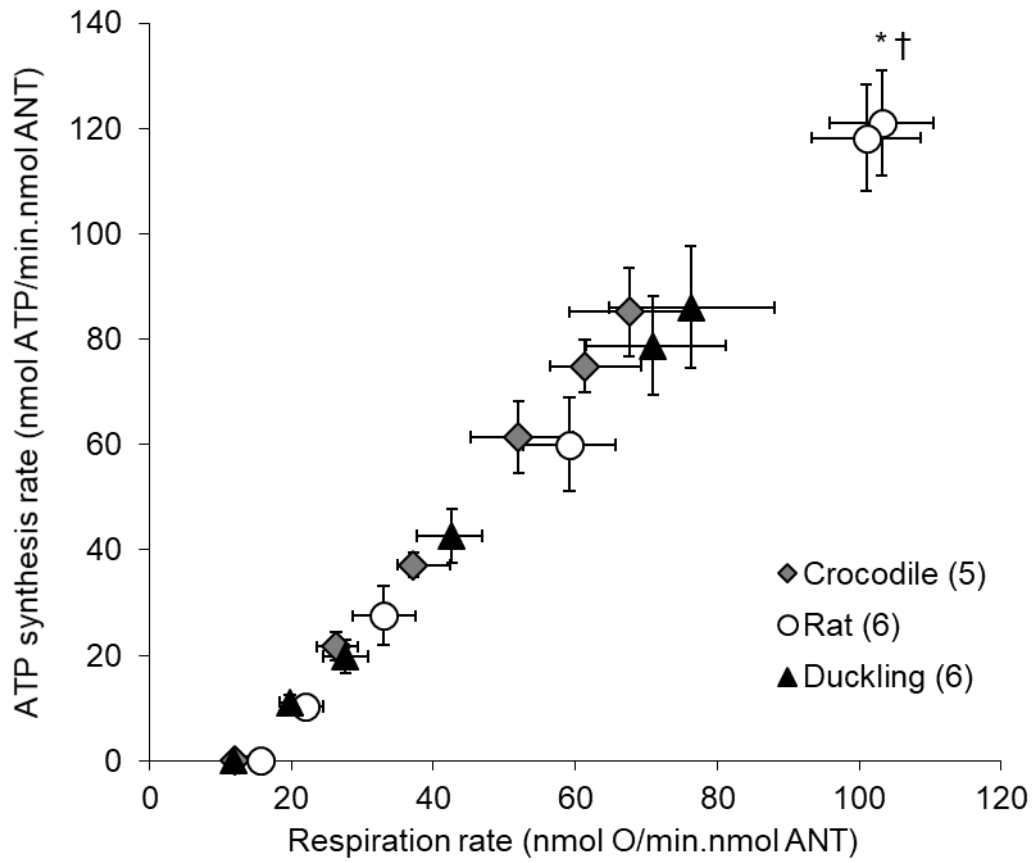


Figure 4



Supplemental Figure 1S

